

AD-A214 047

Office of Naval Research

Report for

1 February 1989 through 1 October 1989

for

Grant Number N00014-89-J-1158
R&T No. 4143117 - 01

Studies of Quantitative Methods for Imaging from
Scattered Fields

Principal Investigator: M. A. Fiddy
Dept. of Electrical Engineering,
University of Lowell,
Lowell, MA 01854

DTIC
ELECTE
NOV 01 1989
S D

DISTRIBUTION STATEMENT A
Approved for public release
Distribution Unlimited

Circulation:
Dr. A. K. Jordan (3 copies)

89 10 27 078

Report

Summary of overall progress

→ The objective of this ~~research~~ project remains ~~that of~~ reconstructing images from scattered field data. ~~We are concerned~~ with targets or objects that cannot be considered weakly scattering, which makes the well known inversion schemes based on the first Born approximation of limited use. Methods based on distorted wave Born and Rytov approximations are under study, as well as techniques which treat the inversion procedure as a spectral estimation exercise. Owing to the difficulty in testing these new procedures with simulated data, due to the inherent difficulty in computing such data sets reliably, ~~we have focused~~ on the use of real data from known simple targets. Work continues on the collection and interpretation of such scattered field data, which has been collected at the RADC Radar Cross Section Facility in Ipswich, MA.

Software has been developed over the last few months, to allow easy manipulation and display of these data sets as well as the images reconstructed from them. We now have the capability of placing each scattered field data set on an arc of arbitrary radius and center in the Fourier domain and then interpolate these data to a cartesian grid; this was important for the evaluation of one of the inversion methods under consideration. Display software has also been developed further, to permit easy image manipulation on screen and hardcopy output onto an LN03 laser printer using binary fill patterns to represent grey scales. The numerical work is currently being carried out on VAX mainframes, via 2000 and 3100 workstations. More details are given below, of the theoretical, numerical and experimental progress and problems encountered during the last six months.

One of the major problems worked on, since the last report was filed, concerns the preprocessing and interpolation of the scattered field data, prior to its use in the various reconstruction algorithms. We have now determined a minimum number of illuminating views necessary to achieve a reliable interpolation, onto a cartesian grid of points, of the Fourier data deduced from the scattered field data. This number is approximately 40 views if no additional limited-view extrapolation algorithms are to be used. We believe that use of the latter is not wise at this stage since their success is questionable and our principal concern is

1
□
□
□
per CS
tes



A-1

of
101

to establish the fundamental information content of the scattered field data. We have arranged to collect a large data set with 40 views during October; this will require use of the RADC chamber for 4 full days.

The scattered field measurements obtained recently have contained some unhelpful artefacts. These data have been noisy at small scattering angles and appear to have suffered both from there being a slight squint associated with the illuminating field and from the consequences of the relatively large diameter of the cylinder used, bringing the detector into the Fresnel region. We have had little success obtaining images from this last data set as will be shown below. Important parameters, such as the cylinder diameter, can be deduced from these data but despite much effort, we have not succeeded in reconstructing a satisfactory image from these data. The next experiment will concentrate on collecting data from more illumination directions, and will revert to a physically smaller cylinder. As more data are collected, we are developing better measurement procedures and checks on the quality of the data.

Preliminary results from the RADC data were presented at the PIERS meeting in Boston in June. A paper has also been submitted for presentation at the RCP 264 Problemes Inverses, to be held in Montpellier, France from Nov. 27th to Dec. 1st of this year. Several theoretical developments have been made but not yet exploited or written up; this will be done during the next few months. One reason for holding back has been our concern over the quality of the experimental data, especially after interpolation.

Technical report

Multiple scattering is assumed from the scattering distribution, i.e. either from $V = V_1 + V_2$ or from the known background component V_1 . We have constructed several targets and collected data from them at 11.242 GHz (or 2.7 cm wavelength). Examples of objects are a 15.24cm diameter cylinder and a 30.48 diameter cylinder each with a rigid base and a height of 5 feet to avoid end effects in the scattering experiments. These cylinders have been filled with sand, sand and empty smaller diameter cylinders acting as "voids" and strongly scattering structures (e.g. metal rods). These cylinders are very heavy when filled with sand, and they have to be firmly mounted onto the turntable in the chamber but in such a way that they can be turned by hand for each new illumination direction. These examples correspond to cylinder diameters of approximately 6 and 12

wavelengths respectively. The product of the wavenumber (k) with the diameter of the target (d) and the magnitude of the scattering potential (V) has to be $kVd \ll 1$ for the first Born approximation to hold and < 1 for the Born series to converge. For these scatterers, kVd is 37 and 75 respectively, when the cylinders are filled with dry sand.

For the geometry of the experimental arrangement, one can assume that the scattered field data are measured in the far field, provided $kd^2/2 \ll z$ (see e.g. J.W. Goodman, Introduction to Fourier Optics, McGraw Hill, 1968, p61). Here, z represents the distance from the center of the target to the detector, which is 3.78 m in this case. The quantity $kd^2/2$ is 2.35m and 9.4m respectively, and hence the approximation that we have far field (Fourier) data for the larger cylinder is not a good one. Indeed, as will be seen below, the scattered field has the features of a Fresnel transform or Fresnel diffraction pattern,) e.g. from a simple aperture, (see for example Ross, G., Fiddy, M.A., Nieto-Vesperinas M and Manolitsakis I, Opt. Acta, 26, (1979) 229-238). As a result, interpretation of the scattered field data as Fourier data requires the incorporation of the appropriate quadratic phase factor for the larger cylinder data. Also, the 30cm diameter cylinder is sufficiently large that some extinction (attenuation) and anomalous diffraction is seen in the forward direction, presumably due to scattering rather than absorption, given the use of dry sand. For both cylinders, forward scattering is stronger than back scattering.

Using these data we have been studying the distorted wave method and comparing reconstructions using this with those obtained using a simple first Born (but not Rytov) inversion scheme. We are relating the scattered field data to Fourier data for V or V_2 . For the Born inversion case, the restricted spatial frequency content of the potential that is calculated, suggests the need for using a spectral estimation procedure that exploits prior knowledge about the background V_1 . Assuming that we have a prior estimate $P(r)$ of the broad features of $V(r)$, eg $V_1(r)$, we can incorporate this spectral estimation method into the inversion scheme as outlined in the original proposal. This estimation procedure is available on the VAX and can be exploited at any time, once the data issues mentioned above are resolved. In principle, one could use the estimation technique to overcome the problem of having only a limited number of illumination directions. However, this estimation method requires a matrix inversion which would be computationally costly and somewhat ill-conditioned for the large size and sparse data sets we have here.

For this reason, it is preferable to take the Fourier data available and interpolate first onto a cartesian grid and then apply the extrapolation procedure if necessary. With Fourier data on a square grid, the method can run much faster and more reliably. This of course puts more significance onto the fidelity of the results of the interpolation routine. To date, we have been evaluating a standard package, namely IQHSCV in the IMSL library. A nearest neighbor algorithm has also been written in order to make comparisons with the IMSL procedure. It was found that the IMSL algorithm was very unreliable in areas of sparse data coverage; it was from a series of experiments with this algorithm that we have now been able to conclude that approximately 40 illumination directions are the minimum necessary to achieve a reliable interpolation using this routine.

Numerical results

The figures shown at the end of this report are as follows:

- 1 the background and scattered field data for the 15.4 cm homogeneous (sand filled) cylinder, (-180° to $+180^{\circ}$)
- 2 the background and scattered field data for the 30.4 cm homogeneous (sand filled) cylinder
- 3 background measured at time of collecting data from 15.4 cm cylinder; this is essentially the incident beam profile
- 4 background measured after collecting data from the 30.4 cm cylinder. The origins of this double peaked incident beam profile are not clear. If it is caused by a beam squint, then this could lead to a reinterpretation of the scattered field data as laterally shifted Fourier data on the potential.
- 5 shows a typical scattered field magnitude data set. The angular spread between maxima of this pattern corresponds to approximately 11.5 degrees. Under the assumption that this scattered field pattern corresponds to Fourier data on the scatterer it should look like a Bessel function, which it does. This angular spread between maxima would correspond to a cylinder of around 15cm diameter; which is correct.
- 6 shows a typical scattered field magnitude form the larger 30.4cm cylinder. This scattered field distribution does not look Bessel-like but does appear somewhat like the Fresnel transform of a cylinder; this is to be expected from the discussion given above concerning the size of this cylinder and the expectation of increased forward scatter. The angular spread between maxima of

- this pattern coincide with those of a Bessel function associated with a cylinder of diameter 30cm.
- 7 this shows the result of taking the Fourier transform of the scattered field with the scattering angle adopted as the Fourier variable; only for sufficiently small scattering angle is this function of an angular variable well approximated by a function of a cartesian variable. If one had Fourier data on a diameter rather than an arc in the Fourier domain, then a Fourier transform of this data would correspond to a projection of the cylinder, which provides a quick estimate, in the domain of the scatterer, of its diameter.
- 8 this is the same as figure 7 but for the larger 30cm diameter cylinder. It is interesting to note that the scattered field data represents Fourier data out to spatial frequencies of $\pm 2k$. One would expect that reducing this k space coverage, would result in a low pass filtering or broadening of these figures 7 and 8, but even truncated down to $\pm 0.25k$ this broadening is not apparent. In this domain, one can therefore identify a window for a low pass filter, which will be useful for smoothing the scattered field data prior to interpolation.
- 9 this pair of figures shows a 15.4cm disk and its associated (128 by 128) Fourier transform magnitude extending to $\pm 1k$.
- 10 this pair of figures shows a 30.4cm disk and its associated (128 by 128) Fourier transform magnitude extending to $\pm 1k$.
- 11 the left figure shows the problem associated with the (IMSL) interpolation routine with sparse data. A sinc function was rotated around the origin and data from this function extracted on 10 semi-circular arcs out to $\pm 1k$. This was to simulate a set of data taken from scattered field measurements for 10 illumination directions. The artefacts in this example are clear, and if the number of illumination directions is increased to approximately 40 (right figure) these artefacts disappear.
- 12 this figure shows the scattered field magnitude from 0 to 180 degrees for the larger 30cm diameter cylinder for one particular illumination direction.
- 13 this shows the phase associated with figure 12 .
- 14 this shows the phase from figure 13 after smoothing using the IMSL routine ICSMOU which smooths by removal of spiked components but with minimal low pass filtering.
- 15 the left hand image shows the scattered field for the larger homogeneous cylinder placed on 40 arcs in the Fourier domain and then interpolated to give the reconstructed image on the right. Data

- were interpolated only out to +/- 1k and the diameter seen for the 30cm cylinder is correct.
- 16 this is similar to figure 15 but for the smaller cylinder; once again, the relative width of the image of the cylinder to that of the reconstruction domain is correct at 15cm in this 128 by 128. For both figures 15 and 16, the data were smoothed prior to interpolation.

The following experimental questions are currently being addressed:

- i) what is the source and nature of noise on the data - is cylinder stability on platform a problem for example?
- ii) can we reduce this noise on the data, especially at low spatial frequencies, (i.e. in the forward direction)?

The following numerical questions are currently being addressed:

- i) should we compare interpolation results with backpropagation?
- ii) what other noise reduction techniques would be more appropriate? (currently we are using the IMSL routine ICSMOU that is a cubic spline method for removing isolated spikes from the data).
- iii) for $kVd \gg 1$, as in our case, we can estimate the error associated with the 1st Born reconstruction using a recently derived relationship between the scattering amplitude and the Fourier data on arcs, which includes an integral term; this will be numerically evaluated with some homogeneous cylinder data.

Future work

The following questions are to be addressed:

- i) our distorted wave technique assumes that the scattering amplitude f_2 associated with the unknown part of the potential $V_2(\mathbf{r})$ is

$$f_2(k\hat{\mathbf{r}}, k\hat{\mathbf{r}}_0) = \int_D \exp(-ik(\hat{\mathbf{r}} - \hat{\mathbf{r}}_0) \cdot \mathbf{r}_1) U(\mathbf{r}_1) d\mathbf{r}_1$$

where f_2 is the scattering amplitude deduced from the data f and the known or calculated f_1 ; this allows one to estimate V_2 from an estimate of U using

$$U(r) = \left(\frac{B_1(r)}{V_1(r)} \right)^2 V_2(r)$$

(see Wombell and Fiddy, *Inverse Problems*, 4 (1988) L23-27). This approach is crude and limited by two problems (at least) but offers a fast method for an improvement over 1st Born. The two problems are limited k coverage rendering B_1 a poor estimate of the 1st Born equivalent object to V_1 and secondly the fact that it is assumed that the approximation to the internal field is satisfactory. The latter really assumes that the product of the potential and the internal field differs only by a rotation from view to view.

ii) We will continue to study the origins of the high pass filtered characteristics of the Born inverted reconstructions, whether they be direct Born inversions of V or distorted wave inversions of V_2 . Preliminary work suggests that incorporation of the prior knowledge about V_1 in the method neglects the fact that the wavenumber associated with ψ_1 is not the free space wavenumber k . We have made theoretical developments based on the assumption of a known homogeneous background, V_1 , with refractive index n , to give the more appropriate wavenumber, nk . Using this, one is forced to reinterpret the relationship of the scattered field data to the Fourier data associated with the scattering object. It seems that the semi-circular arcs on which Fourier data are collected remain of radius k but now have center nk leading to a region around the k origin without data.

Through theoretical work and numerical experiments, we expect to show that this can explain the high pass filtered characteristics of the reconstructions when the data are not appropriately shifted.

If one works with f_2 rather than f , the Fourier data should be on arcs of radius nk and centered at nk . An application of this is that of determining the value of n for a near homogeneous object by sliding the data on arcs of radius k to different centers, in order to see how the recovery of the homogeneity alters.

The problem with arc shifting is that implicitly assumes that a plane wave is a good approximation to the internal field for all views; this is in the spirit of the distorted wave approach. This can be extended to the case for which there are two plane waves used to model the internal field and given the data relationship to the associated arcs. indeed, the coefficients of an angular spread of plane waves representing the internal field could be found for each view. From this information, one would know the internal field and thus be able to solve

$$f(k^{\wedge}_L, k^{\wedge}_{L_0}) = \int_D \exp(-ik^{\wedge}_L \cdot r_1) V(r_1) \psi(r_1, k^{\wedge}_{L_0}) dr_1$$

or

$$f_1(k^{\wedge}_L, k^{\wedge}_{L_0}) = \int_D \exp(-ik^{\wedge}_L \cdot r_1) V_1(r_1) \psi_1(r_1, k^{\wedge}_{L_0}) dr_1$$

$$f_2(k^{\wedge}_L, k^{\wedge}_{L_1}) = \int_D \psi_1(r_1, -k^{\wedge}_L) V_2(r_1) \psi(r_1, k^{\wedge}_{L_0}) dr_1$$

iii) Our motivation remains that of developing a procedure which remains computationally straightforward in order to allow easy comparisons to be made between reconstructions with known objects using real data. The following directions are to be pursued:

a) numerical studies of the following alternative approach to deduce the actual internal field ψ for an arbitrary scatterer

$$f(k^{\wedge}_L, k^{\wedge}_{L_0}) = \int_D \exp(-ik^{\wedge}_L \cdot r_1) V(r_1) \psi(r_1, k^{\wedge}_{L_0}) dr_1$$

$$f(k^{\wedge}_L, k^{\wedge}_{L_0}) = \int_D \exp(-iK \cdot r_1) U(r_1, k^{\wedge}_{\alpha}) \psi_0(r_1, k^{\wedge}_{\alpha}) dr_1$$

Knowledge of $\psi_0(r_1, k^{\wedge}_{\alpha})$ and calculation of an optimal BPDFT estimate for an effective Born potential $U(r_1, k^{\wedge}_{\alpha})$, (ie source term), from the scattered field data, allows the scattered field, ψ to be computed anywhere including in D for each illumination direction. This means that we could estimate $\psi(r_1, k^{\wedge}_{L_0})$, leaving the total potential or object function $V(r_1)$ as the only unknown in the identity

$$U(r, k^{\wedge}r_0) \psi_0(r, k^{\wedge}r_0) = V(r) \psi(r, k^{\wedge}r_0)$$

We can compare reconstructions obtained in this manner with the known object structure and thus evaluate the usefulness of the approach.

b) From calculating a set of functions $U(r, k^{\wedge} r_0) \psi_0(r, k^{\wedge} r_0)$ from the scattered field data (using the PDFT if necessary) we can use this equivalence, namely

$$U(r, k^{\wedge} r_0) \psi_0(r, k^{\wedge} r_0) = V(r) \psi(r, k^{\wedge} r_0)$$

one could extract V from the ensemble of products available from all the illumination directions used. One can use a bispectral reconstruction method, which is designed to take an ensemble of image frames representing an unknown image convolved with a set of essentially random (atmosphere) point spread functions and recover the image. For sufficiently complicated and large scatterers, V , we will consider the internal field as essentially random from view to view. The product $V(r) \psi(r, k^{\wedge} r_0)$ is already in the "spectral domain" in this context, from which the bispectrum can be easily calculated.

Publications and presentations since Feb. 1st 1989

Alavi, A., F. C. Lin, M.A. Fiddy, and C.L. Byrne, "Image estimation from scattered field data (at 10GHz) using the distorted wave Born approximation and other prior knowledge", submitted to R.C.P. 264, Problemes Inverses, Montpellier, Dec. 1989.

Alavi, A., F. C. Lin, M.A. Fiddy, R.J. Wombell and C.L. Byrne, "Imaging from limited scattered field data in the distorted wave Born approximation", submitted to P.I.E.R.S. Meeting, Cambridge MA, July 1989, 416-417.

Fiddy, M.A., "Inversion of optical scattered fields and image reconstruction", Prtoc. NSF Panel on Scattering and Inverse Scattering Theories in Workshop on Future Directions in Electromagnetics Research, 4pp, July 26, 1989.

Abbiss, J.B., B.J. Brames and M. A. Fiddy, "Super-resolution algorithms for a modified Hopfield neural network", submitted to IEEE Trans ASSP.

Domash, L, P. Leven and M. A. Fiddy, "Fluctuation interferometer as high angular resolution sensor of laser illumination", Proc. 6th Rochester Conference on Coherence and Quantum Optics, Digest of Abstracts, pp117-119, (full paper to appear in volume published by Plenum Press).

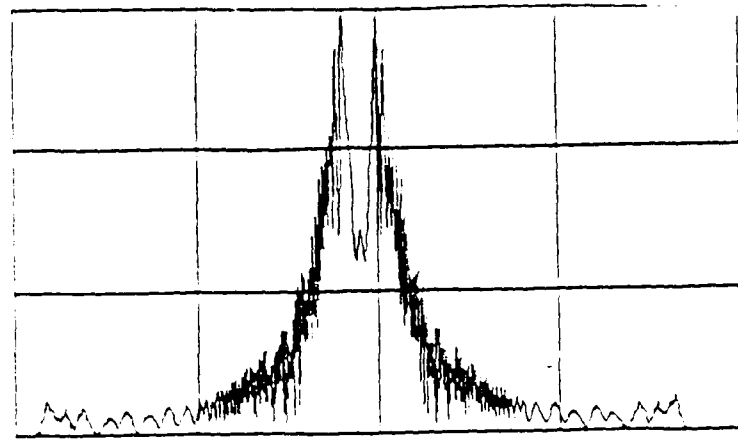
Fiddy, M.A., J.D. Newman, R.C. Van Vranken and D.L. Clark, "Imaging of moving objects through random media, from low light level noisy data", submitted to Opt. Soc. Amer. Topical Meeting on Quantum Limited Imaging and Information Processing II, Cape Cod, June 1989, pp87-89.

Leon, R., Lin F.C. , Walker, N.P., D.R. Drury and M.A. Fiddy, "Optical bistable switch based on self-focusing in artificial Kerr medium", Opt. Soc. Amer. Topical Meeting on Photonic Switching, Salt Lake City, March 1st to 3rd, 1989, pp35-36.

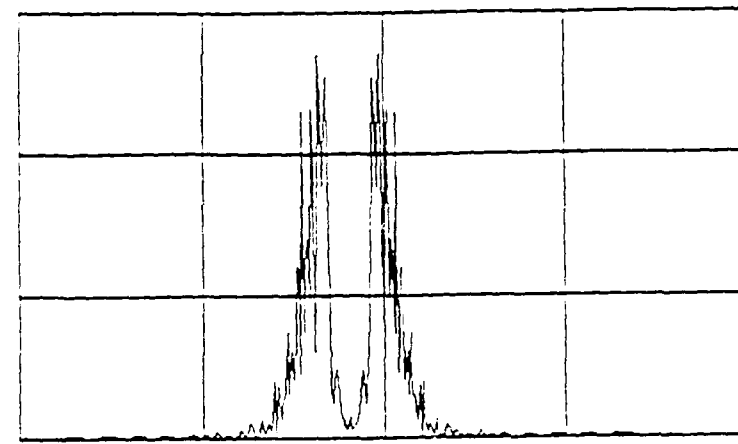
Brames, B.J. and M.A. Fiddy, "Reconstruction of two dimensional signals from nonuniform samples or partial information: comment", J. Opt. Soc. Amer. A6 (1989) 1308-1309.

Walker, N.P. and M.A. Fiddy, "An efficient optical bistable device based on self-focusing", Appl. Opt., 28, Feb. 1989 issue.

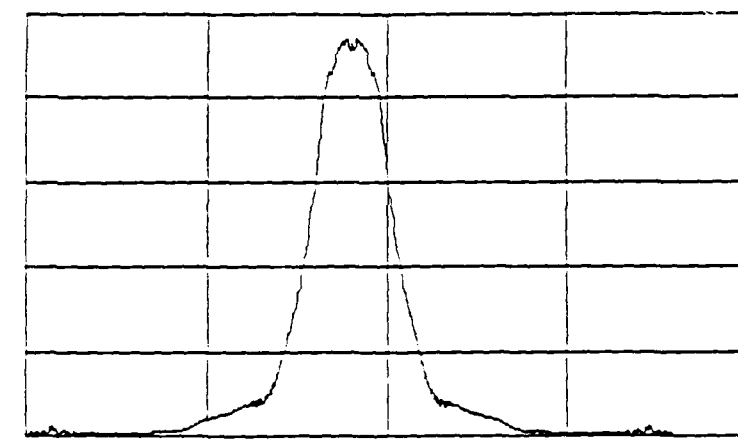
Fiddy, M.A., J.B. Abbiss and B.J. Brames, "On the application of neural networks to the solution of image restoration problems", in High Speed Computing II, Ed. K. Bromley, Proc. SPIE 1058, pp 138-146 , 1989.



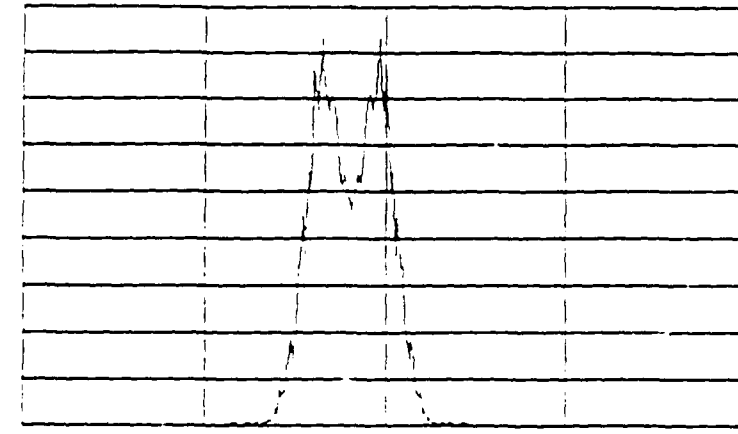
2



3



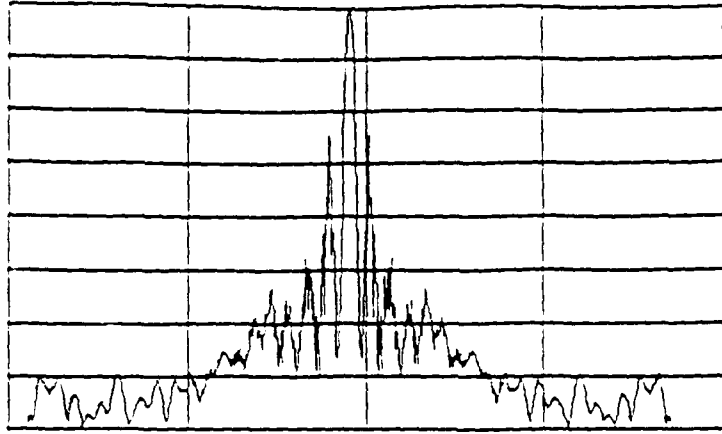
4



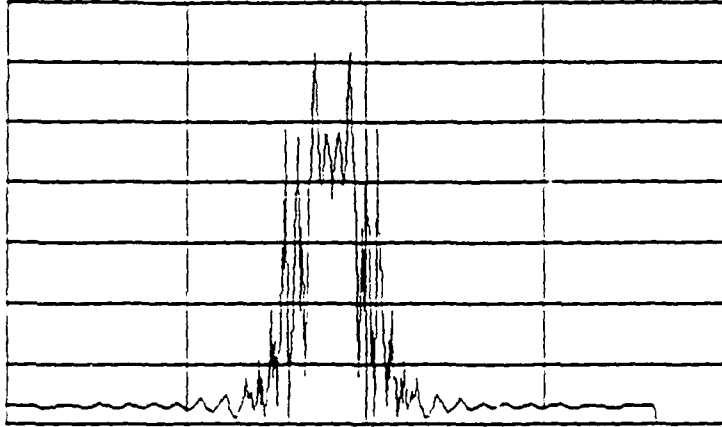
↑
-180°

↑
180°

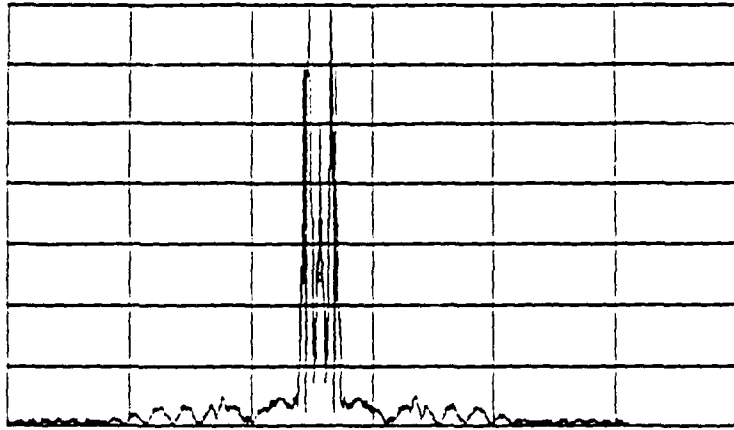
5



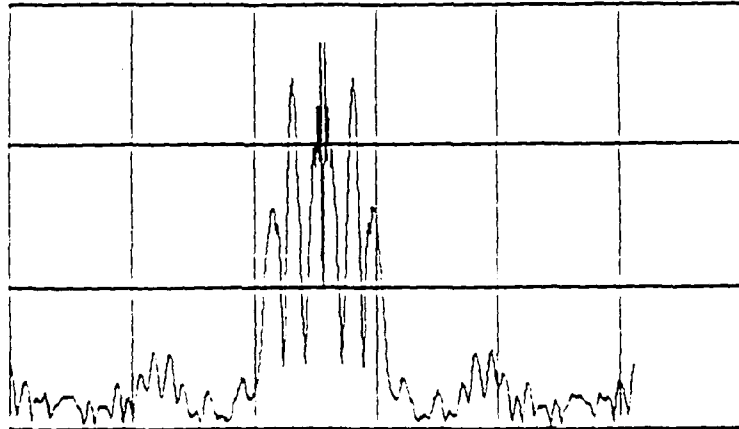
6

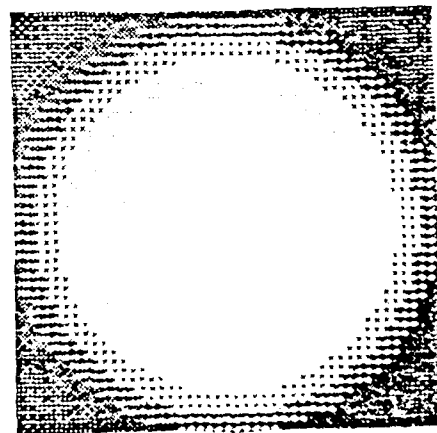
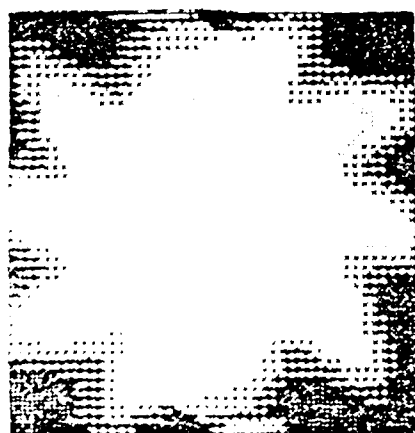
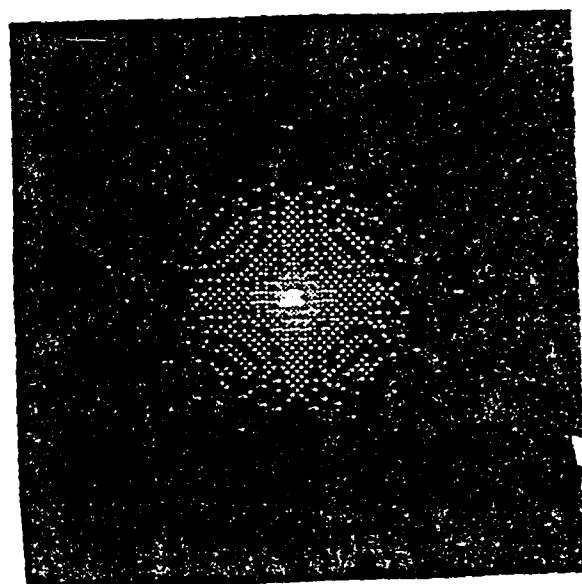
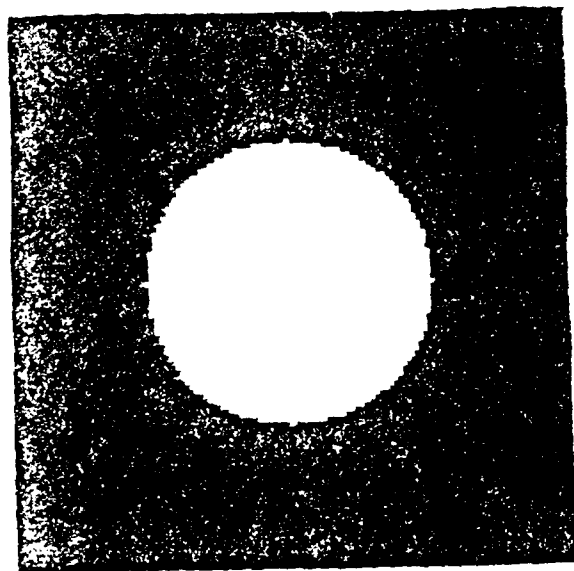
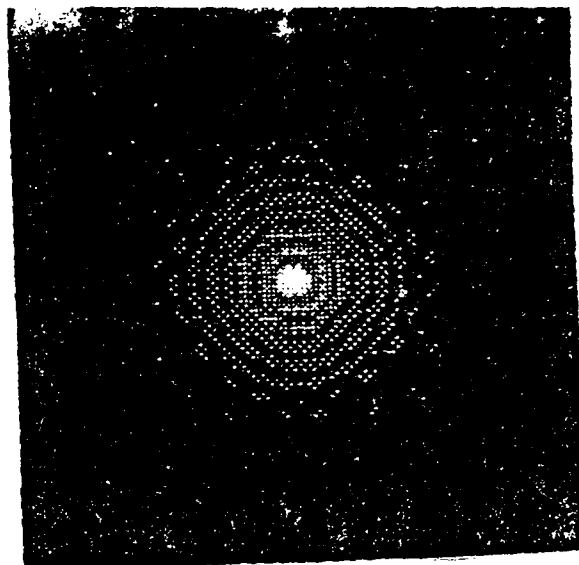
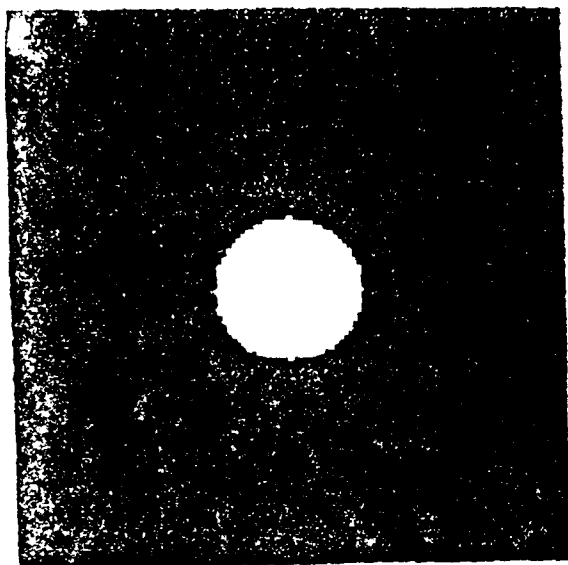


7

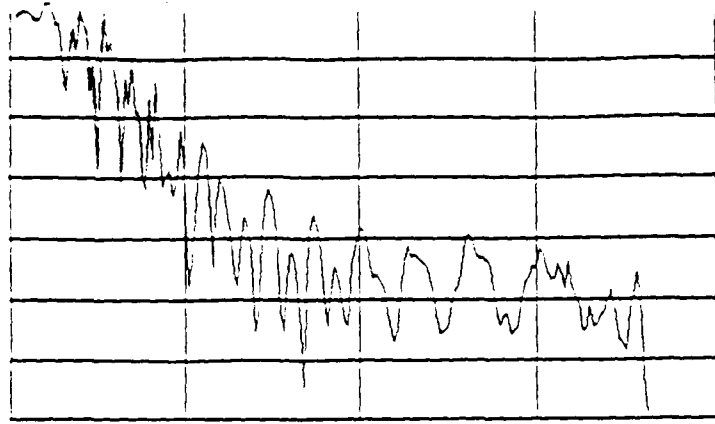


8

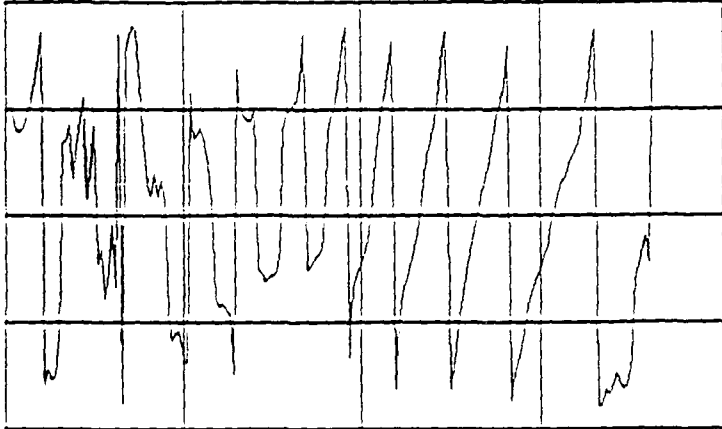




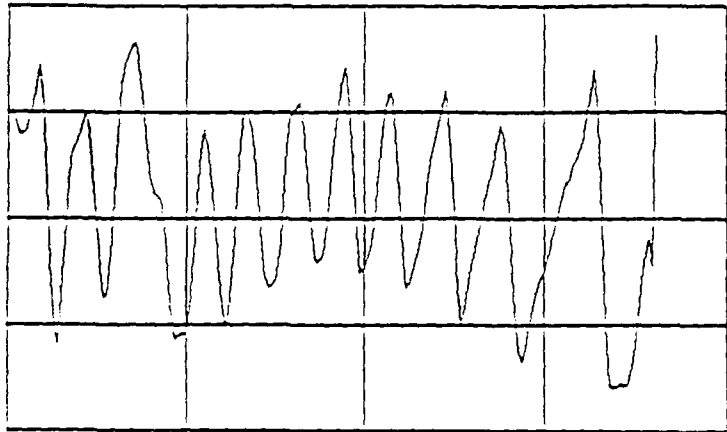
12



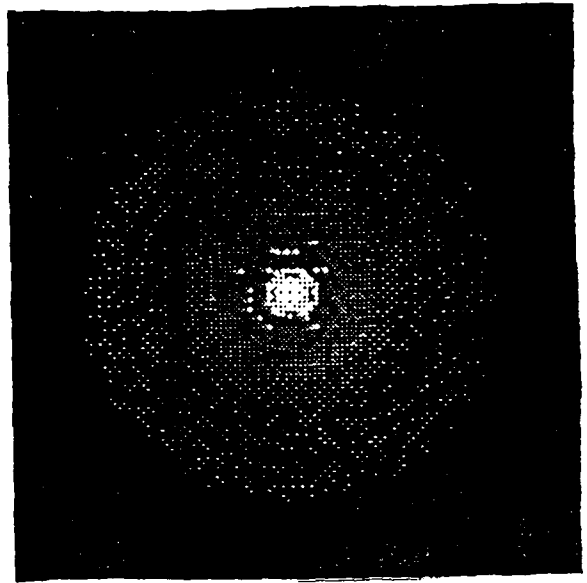
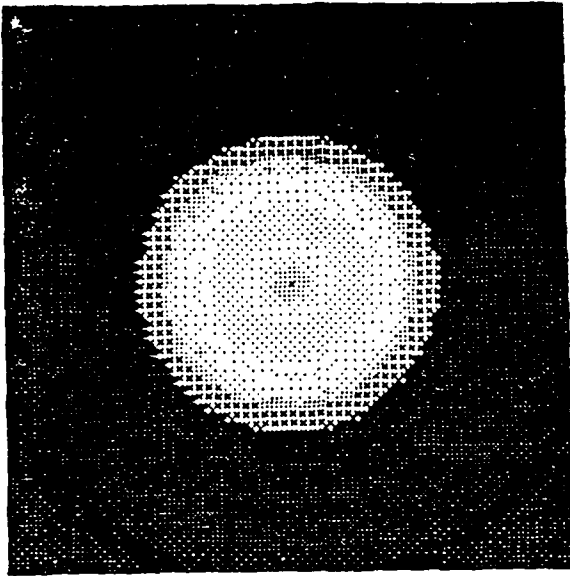
13



14



15



16

